UDC 621 . 624 . 154 / . 155 : 669 . 14 - 462

A Study of the Screwed Pile –The Results of Installation and Loading Tests and Analysis of Penetration Mechanisms–

Eiichiro SAEKI*1 Hitoshi OHKI*1

Abstract

Installation and loading tests of mid-size screwed steel pipe piles were executed, and the following results were obtained. 1) It is possible to drive them into and through sand layers having 50 to 70 STP N-values, with no discharge, noise nor vibration. 2) The characteristics of pile penetration are influenced by spiral wing diameter, angle and shape. 3) There is a strong correlation between bearing capacity and torque and it is possible to estimate the capacity from the R_p-value proposed in this paper.

1. Introduction

Piling is the most common foundation construction method for structures on soft ground. Pile foundations can be classified into main types as shown in **Fig. 1**. These pile foundation construction methods have specific characteristics as described below. Driven piles are highly reliable as to the end bearing capacity, but produce such environmental problems as noise and vibration and thus are no longer used in cities or in nearby areas. Cast-in-place piles and bored precast concrete piles do not cause noise and vibration problems, but require the disposal of muddy water and surplus soil. These waste materials have been posing a social problem in recent years. Cast-in-place piles are installed by forming holes in the ground and then filling them with concrete. The slime produced in this process must be disposed of, and the end bearing capacity is difficult to check.

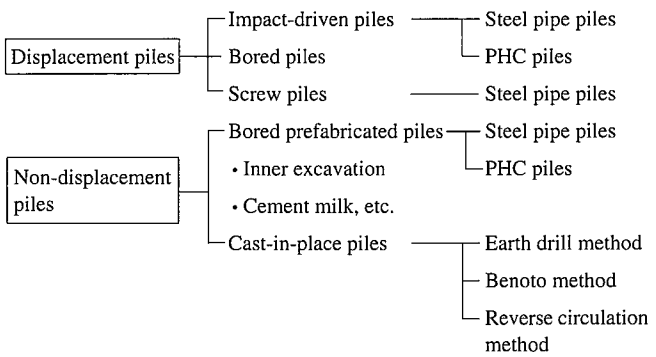

Fig. 1 Classification of pile foundation construction methods

The screw piling method was formerly used as an effective means, for manually installing piles in Japan. At the advent of diesel hammers, however, the screw piling method lost its economic advantage and is now rarely used in Japan, except for small-diameter screw piles for residential construction[1-4].

This paper presents the study results of screw steel pipe piles expected to provide solutions to the problems of conventional piling methods.

2. Installation and Features of Screw Steel Pipe Piles

The screw steel pipe pile (hereinafter referred to as the screw pile) is a steel pipe with a spiral blade fixed at its lower end as illustrated in **Fig. 2**. Using a pile driver or the like, the screw pile is given a vertical downward or upward load and a rotating torque, and is twisted into the ground with the wedge effect of the blade utilized as the driving force. The screw piles feature the following:

1) They are classified as displacement piles and are expected to provide a large bearing capacity due to the base enlargement effect of the blade.
2) They are expected to develop a large uplift bearing capacity due to the anchor effect of the blade.
3) The bearing capacity of every pile can be checked according to

*1 Building Construction Division

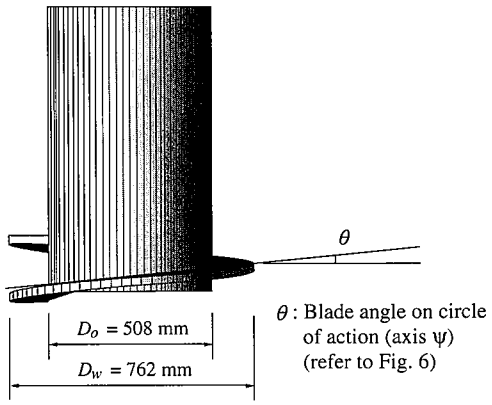

Fig. 2 Shape of test pile (with one blade)

construction records such as torque, and the finish of their screwing can be controlled easily and accurately.

4) They produce no surplus soil, muddy water, and other waste materials at all.
5) They can be easily pulled out by turning them in the reverse direction.
6) They have excellent deformation capacity, strength, and seismic performance.

3. Purposes of Study

This study has the following purposes:

1) Check whether or not medium-diameter piles in the diameter range of 300 to 600 mm, can be screwed in ordinary Japanese.
2) Extract and analyze blade shape parameters that affect the installation of screw piles.
3) Determine the bearing capacity characteristics of screw piles.
4) Clarify the relationship between the end bearing capacity and screwing properties (mainly torque) of screw piles.

4. Outline of Test Site

The test sites were situated in Futtsu City, Chiba Prefecture, and in reclaimed land at the center of the Boso Peninsula and along the Tokyo Bay. The subsurface investigation results are shown in **Fig. 3**. The strata are composed as described below, starting with the surface layer.

(1) 0.00 to 1.30 m: Backfill stratum (secondary sedimentary stratum)

This stratum is classified as a secondary sedimentary stratum and is mainly composed of coarse sand with many scattered shell pieces.

(2) 1.30 to 2.70 m: Alluvial sandy soil stratum

This is a greenish gray fine sand stratum and has shell pieces scattered because it is also a marine stratum. The N-value ranges from 8 to 10, indicating a slightly low degree of consolidation.

(3) 2.70 to 5.70 m: Alluvial cohesive soil stratum

Yellowish brown sandy silt is deposited, and the N-value is 1 to 2, indicating a soft state.

(4) 5.70 to 12.90 m: Diluvial-alluvial sandy soil stratum

This stratum was deposited from the end of the Pleistocene to the start of the Holocene.

5.70 to 8.60 m: Fine sand layer with N-value of 21 to 29 (inter mediate layer)

8.60 to 10.80 m: Silty, fine sand layer with N-value of 7 to 9

10.80 to 12.90 m: Medium sand layer mixed with fine gravel,

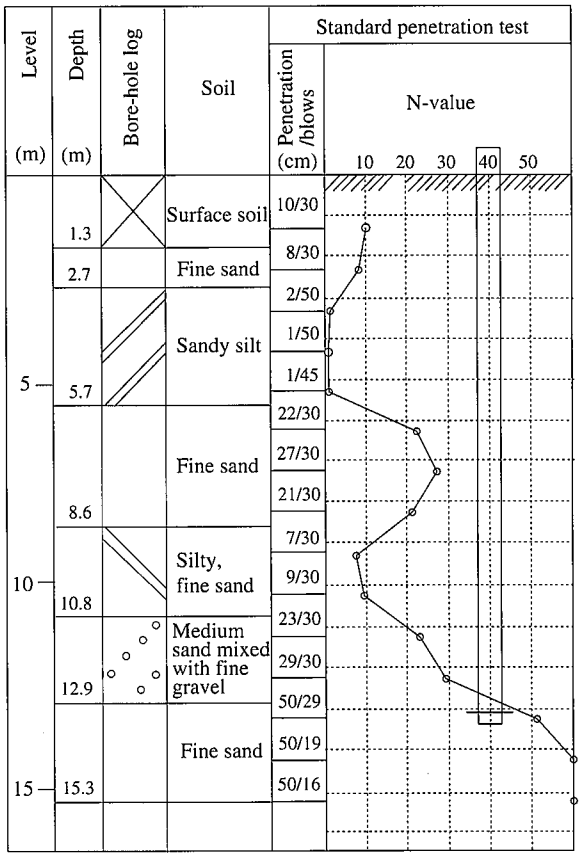

Fig. 3 Boring data

having N-value of 21 to 29

(5) 12.90 to 15.31 m: Diluvial sandy soil stratum

Dark gray and well-compacted fine sand is distributed. This stratum exhibits an N-value of 50 or over and is highly compacted. It can be regarded as the bearing stratum.

5. Installation Test Types and Installation Machinery

In the screw piling method, the end shape of screw piles has a large influence on the installability of the screw piles. The following can be considered as parameters:

1) Diameter of steel pipe body
2) Shape of blade
3) Outside diameter of blade
4) Pitch of blade (elevation change per rotation)
5) Open-end ratio of bottom plate portion of steel pipe body (refer to "Definition of terms" at the end of the paper)

Full-size screw piles were installation tested to determine the effects of these five items on the installability of the screw piles.

Table 1 lists the test specimens. The standard pile had the steel pipe diameter D_o of 508.0 mm, two blades with the diameter D_w of $1.5D_o$ and angle of 5°, and the open-end ratio of 90%. The effect of each parameter was evaluated by the test results of all of the 24 specimens. All but some specimens were tested twice each. A specimen is schematically illustrated in **Fig. 2**. A pile driver (Nippon Sharyo Model DH-658M) was used as the base pile installation machine, and an earth auger (Sanwa Kizai Model SMD-150H) was used as the driving machine.

Table 1 List of test piles

Test pile	Steel pipe diameter D_o (mm)	Blade shape	Blade diameter ratio D_w/D_o	Open-end ratio (%)	Blade angle depth θ (deg)	Embedment GL–(m)		Remarks
1 5W15M09	508	2 blades	1.5	90	5	13.7	11.6	Standared pile
2 5S15M09		1 blade				13.7	13.7	
3 5W12M09			1.2			7.6		
4 5W20M09			2.0			13.5	13.5	
5 5W15M07				70		11.5	14.0	
6 5W15M00				0		13.3	12.0	
7 5W15S09					2.5	11.7	13.7	
8 5W15D09					10	13.0	13.7	
9 5S15M00		1 blade		0		13.4	13.4	
10 5S15M10		1 blade		100		13.7	13.4	
11 5W15D10				100	10	13.1		
12 5W15D10-B				100	10	13.0	13.0	With excavation bit
13 5W17M09			1.75			13.8	13.7	
14 5S15MBL		1 blade				13.6		Bottomless
15 6W15M09	609.6	2 blades	1.5	90	5	16.4	14.2	
16 6W15S09					2.5	16.4	14.0	
17 6W15D09					10	16.4	14.0	
18 6S15M00		1 blade		0		16.4		
19 6S15M10		1 blade		100		16.4	13.5	
20 6S15D09		1 blade			10	16.4		
21 3W15M09	318.5	2 blades	1.5	90	5	15.0	15.0	
22 3W15M07				70		17.5	15.5	
23 3S15M00		1 blade		0		16.2		
24 3S15M10		1 blade		100		16.8		

Data in blank spaces are same as those of standard pile (5W15M9).

6. Measurement Items and Methods

The measurement items and methods of screw pile installation data are described below.

1) Applied load

A vertical load was applied to a screw pile during installation. It was divided into downward and upward components. The upward load was measured with a load cell set between the wire used to lift the earth auger and the top of the leader. The downward load was measured with a load cell set at the end of wire used to pull down the earth auger (as normally done under the inner excavation method).

2) Torque

The motor current was measured and converted to a corresponding value of torque.

3) Penetration

The penetration of the screw pipe per rotation was measured and was also converted from the penetration rate.

4) Penetration rate

The feed rate of the earth auger lifting wire was measured as the penetration rate of the screw pile.

5) In-pipe soil elevation

The elevation of soil in the steel pipe was measured with a plumb bob when the pile end reached desired depth or was installed to 5, 8, 10 or 12 m below the ground level, or when the installation of the pile was stopped.

7. Results of Installation Test

Typical results of the installation test are shown in **Fig. 4**. The measurement items are shown for two specimens. Or the torque (kN·m), penetration per rotation (mm/rotation), applied load (kN), and in-pipe soil elevation (m) are shown from left to right. The Y-axis indicates the penetration of the end of each screw pile. The penetration characteristics of the screw piles greatly depend on the blade shape parameters. Particularly where the N-value suddenly increased, the screw piles greatly differed in their penetration, and some screw piles were not driven any further.

In each case, the penetration torque exhibited a good correlation with the N-value. The screw pile penetrated through a soft soil with relatively small torque. In the intermediate strata and the bearing stratum, the torque changed with the hardness of the soil encountered. The torque increased with increasing pipe diameter (blade diameter), indicating the effect of the pile area or volume. As the effect of the end shape, a single blade required a larger torque than two blades, but provided a larger penetration per rotation. The torque increased with increasing blade diameter and angle, and decreased with decreasing blade diameter and angle. The slip phenomenon that the penetration became practically zero was found to occur ahead of an intermediate stratum when the blade diameter ratio was 1.2 and ahead of the bearing stratum when the blade angle was 2.5°.

The penetration per rotation can be controlled by changing the applied load. The screw pile can penetrate through soft soil by an amount approximately equal to the blade pitch, but cannot penetrate through hard soil by such a large amount. When the end resistance increases during a change from soft to hard soils, the slip phenomenon sometimes occurs. Application of load increases the pressure imposed on the bottom plate portion and facilitates the penetration of the pile into hard soil. The applied load-depth curve indicates how

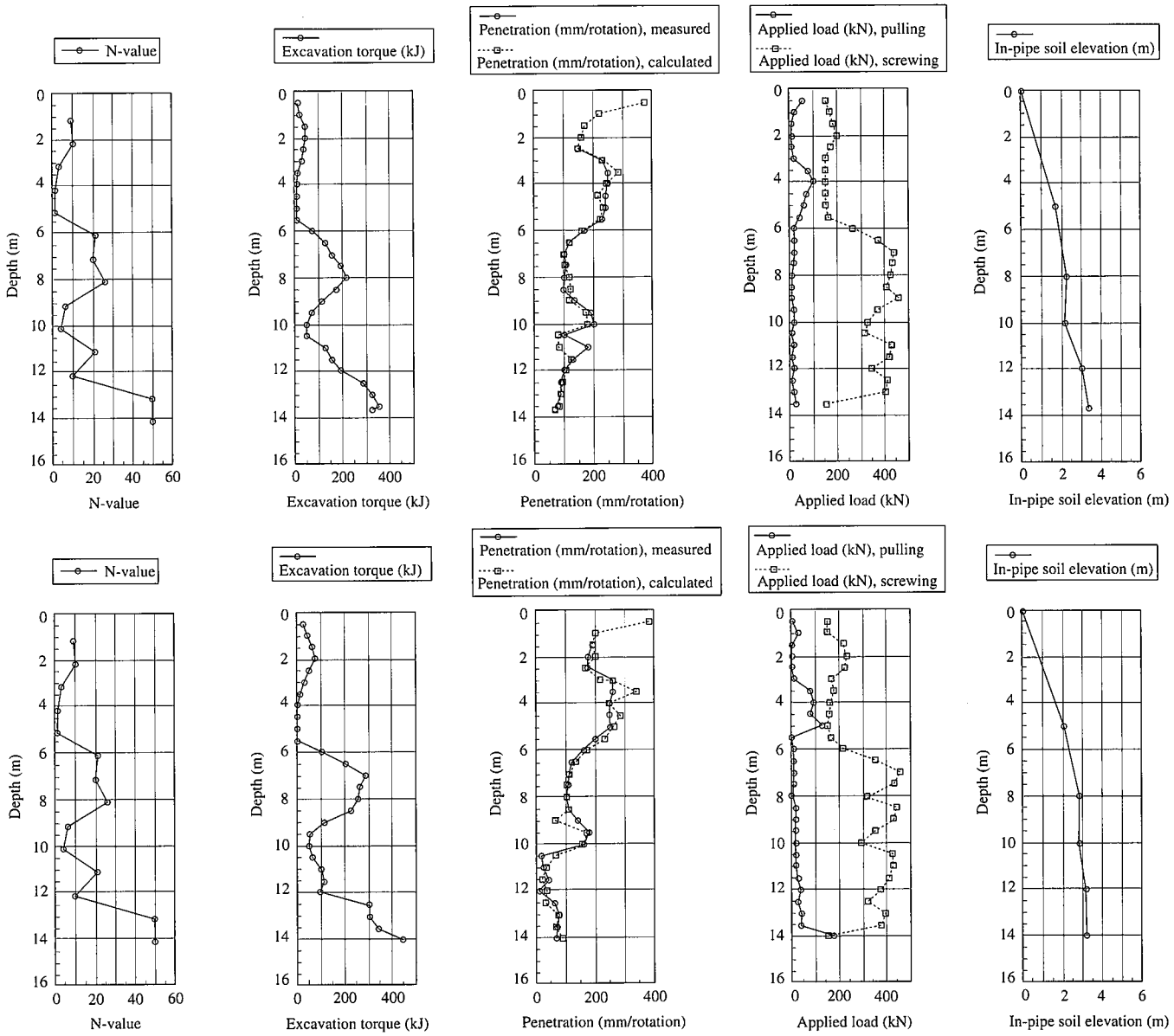

Fig. 4 Installation record (upper row: 5S15M10-1, lower row: 6S15M10-1, two piles with same N-values)

the load was applied to the pile at each depth. The applied load includes the dead weight of the earth auger (151.9 kN).

The in-pile soil elevation does not uniformly increase in the depth direction. The level of the soil in the pipe increases as the screw pile penetrates through a hard soil with a large end reaction as in the intermediate or bearing stratum. This may be taken to mean that additional soil enters the pipe when the end reaction of soil to the pile end exceeds the resultant of the static frictional forces between inside wall of the pipe and the soil preexisting in the pipe. **Photo 1** shows the condition of soil in a screw pile withdrawn after installation and longitudinally halved. This photo confirms the above-mentioned phenomenon. The in-pipe soil elevation increases with increasing pipe diameter.

According to the test results discussed above, it was found that when the end of a screw pile is shaped to ensure good penetration, the soil conditions at the pile end during installation can be practi-

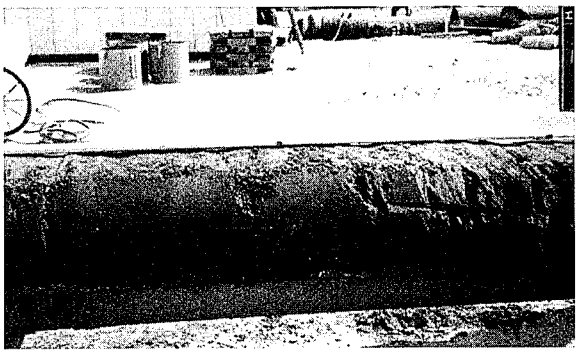

Photo 1 Soil in steel pipe (609.6 mm diameter)

cally grasped by torque control and that the blade diameter and angle affect the installability of the screw pile.

8. Penetration Mechanism of Screw Piles

8.1 Force equilibrium at pile end during penetration

The screw piling method twists the steel pipe body of the screw pile so that the blade at the lower end of the screw pile excavates the soil and pushes up the soil. The resultant driving force causes the penetration of the screw pile into the ground. When the screw pile is handled as a closed-end pile, this phenomenon is explained below according to the equilibrium of forces.

Th axis ψ on the circle of action shown in **Fig. 5** is linearly developed in **Fig. 6**. **Fig. 6** shows the model of the blade excavating and penetrating the soil encountered. **Fig. 7** illustrates the equilibrium of forces acting on the blade and bottom plate where θ is the blade angle, η is the penetration angle, and T_b is the torque acting at the pile end (refer to "Nomenclature" at the end of the paper). This equilibrium of forces is shown in vector form in **Fig. 8**, and is mathematically expressed by the following equations where H_t is the torque

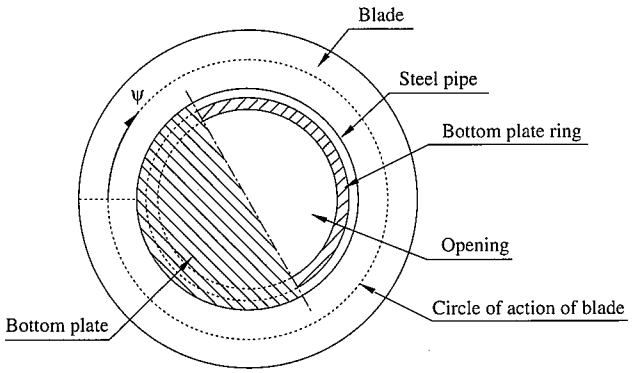

Fig. 5 Plan of screw pile (concerning axis ψ)

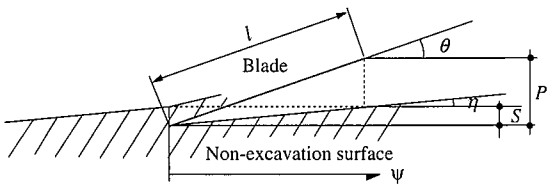

Fig. 6 Relationship between non-excavation surface on axis ψ and blade in steady state

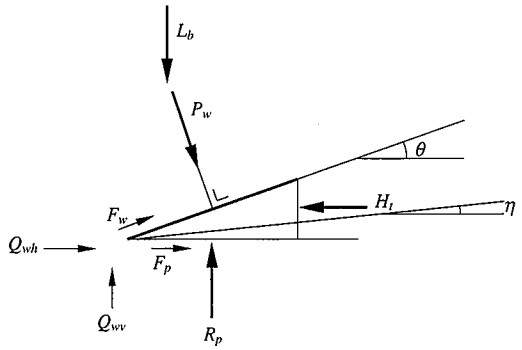

Fig. 7 Forces acting on blade and bottom plate

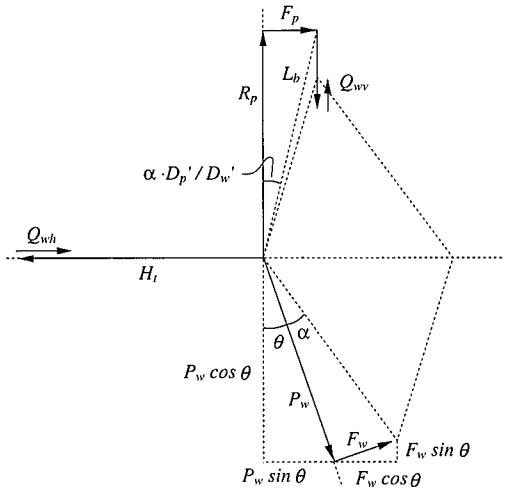

Fig. 8 Equilibrium of forces (vector diagram)

converted into an equivalent force on the circle of action (axis ψ).

$$H_t - Q_{wh} = F_p + P_w \sin\theta + F_w \cos\theta \quad (1)$$

$$R_p - L_b + Q_{wv} = P_w \cos\theta - F_w \sin\theta \quad (2)$$

Elimination of P_w from Eqs. (1) and (2) allows R_p to be expressed as a function of the torque as follows:

$$R_p = \frac{(\cos\theta - \alpha\sin\theta)(H_t - Q_{wh}) + (\sin\theta + \alpha\cos\theta)(L_b - Q_{wv})}{\sin\theta + \alpha\cos\theta + \alpha(D_p' / D_w')(\cos\theta - \alpha\sin\theta)} \quad (3)$$

where,

$F_p = \alpha(D_p' / D_w')R_p$

$F_w = \alpha P_w$

8.2 Mechanism of penetration

The screw pile penetrates while rotating, but does not always penetrate at the blade pitch P (elevation change per rotation) like screws. This is because the excavated soil, which is an elastic-plastic material, is pushed upward to obtain the penetration force. To represent this phenomenon, the soil above the blade of a screw pile penetrating into the uniform ground and below the bottom plate portion of the screw pile is assumed to be an elastic-plastic spring as shown in **Fig. 9**. The equilibrium of forces acting on the screw pile penetrating into the ground in a steady state cane be illustrated as shown in **Fig. 10**.

From the equilibrium of forces shown in **Fig. 11** $R_p = f_w + L_b$ (with the bit edge resistance ignored), when the soil on the blade surface undergoes elastic deformation or $P - S \le \frac{Q_{ys}}{K_s}$, the equilib-

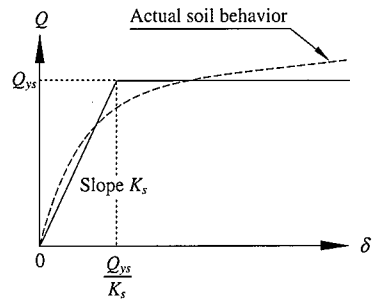

Fig. 9 Dynamic characteristics of soil (as elastic-plastic spring)

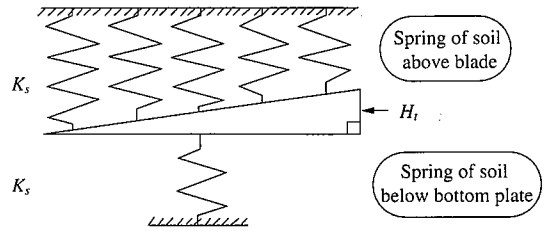

Fig. 10 Equilibrium of forces acting on blade

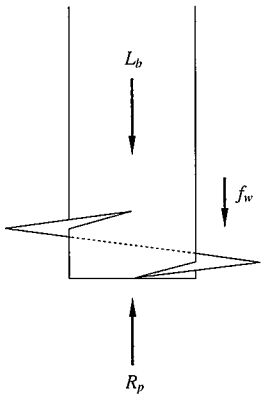

Fig. 11 Equilibrium of forces acting on pile end

rium of forces acting on the blade is given by

$$A_p Q_{ys} = A_w \frac{K_s(P-S)}{2} + L_b \tag{4}$$

From this, S is obtained as follows:

$$S = P - \frac{2A_p Q_{ys} - 2L_b}{A_w K_s} \tag{5}$$

When the soil on the blade surface undergoes elastic-plastic deformation or $P - S > \frac{Q_{ys}}{K_s}$, the equilibrium of forces acting on the blade is given by

$$A_p Q_{ys} = \frac{Q_{ys}}{2} A_w \frac{Q_{ys}}{K_s(P-S)} + Q_{ys} A_w \left(1 - \frac{Q_{ys}}{K_s(P-S)}\right) + L_b \tag{6}$$

From this, S is obtained as follows:

$$S = P - \frac{A_w {Q_{ys}}^2}{2K_s(A_w Q_{ys} - A_p Q_{ys} + L_b)} \tag{7}$$

It is thus theoretically clear that irrespective of the whether the soil encountered is elastic or elastic-plastic, the screw pile penetrates through the soil by an amount smaller than the blade pitch when there are the second terms in Eqs. (5) and (7) and when L_b is small. From Eqs. (5) and (7), when $L_b = 0$, the condition A_p/A_w for the elastic behavior of the soil is given by

$A_p/A_w \leq 0.5$

When $L_b = 0$, the condition A_p/A_w for the elastic-plastic behavior of the soil is given by

$A_p/A_w > 0.5$

From Eq. (7), when $A_p/A_w = 1 - Q_{ys}/2PK_s$,

$S = 0$

When A_p/A_w is larger than the value of S (or the blade area ratio A_w/A_p is smaller than the reciprocal of the value s) and when $L_b = 0$, the screw pile does not penetrate through a uniform soil.

9. Evaluation of Penetration Resistance by Energy Equilibrium and End Bearing Capacity

9.1 Evaluation of Penetration Resistance by Energy Equilibrium

Like the equilibrium of forces, the equilibrium of input energy and consumed energy allows the correlation between the torque and penetration resistance to be obtained and the end bearing capacity to be estimated.

Assuming that the screw pile is rigid as shown in **Fig. 12** and ignoring as an infinitesimal term the directional cosine that depends on the blade shape and pile penetration condition, the energy input to the pile head per rotation is the sum of the energy ($L_t S$) input by the applied load and the energy ($2\pi T_t$) input by the torque. The energy consumed in the bottom plate portion is the sum of the energy ($R_p S$) consumed by pile penetration in the bottom plate portion, the energy ($\alpha R_p \pi D_p'$) consumed by friction of the bottom plate portion, the energy ($\alpha(R_p - L_b + Q_{wv})\pi D_w'$) consumed by friction of the blade upper surface, the energy ($(R_p - L_b + Q_{wv}) \times (P - S)$) consumed by the soil due to the upward forced deformation of the blade, the energy ($Q_{wh}\pi D_w'$) consumed by horizontal bit edge resistance, and the energy ($Q_{wv}S$) consumed by vertical bit edge resistance (refer to **Fig. 7**).

Let a be the transfer ratio that takes into account the energy consumed by the skin friction during installation of the screw pile. Then, from the equilibrium of the input energy and consumed energy,

$$\begin{aligned} a(L_t S + 2\pi T_t) &= L_b S + 2\pi T_b \\ &= R_p S + \alpha R_p \pi D_p' + \alpha(R_p - L_b + Q_{wv})\pi D_w' \\ &\quad + (R_p - L_b + Q_{wv})(P - S) + Q_{wh}\pi D_w' + Q_{wv} S \end{aligned} \tag{8}$$

and

$$R_p = \frac{2\pi T_b + L_b(\alpha\pi D_w' + P) - Q_{wh}\pi D_w' - Q_{wv}(\alpha\pi D_w' + P)}{\alpha\pi(D_p' + D_w') + P} \tag{9}$$

9.2 Estimation of end bearing capacity

When the penetration S is equal to the blade pitch P as shown in **Fig. 13**, the pile end is not affected by the blade, and the penetration

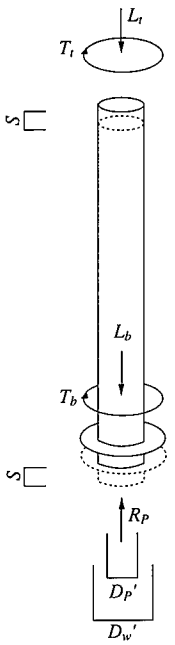

Fig. 12 Model for energy equilibrium

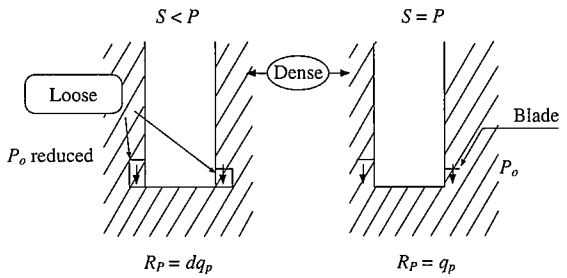

Fig. 13 Penetration and soil condition at pile end

resistance R_p of the pile end is equal to the ultimate bearing capacity q_p of the bottom plate portion. When $S < P$, the blade loosens the soil around the bottom plate portion, and the effective stress of the lower part of the blade diminishes. As a result, R_p is considered to be reduced to dq_p (d is the penetration resistance reduction factor.)

The end bearing capacity is expressed by Eq.(10) as the sum of the penetration resistance of the bottom plate portion and the bearing capacity of the blade (area ratio multiple of the penetration resistance of the bottom plate portion multiplied by the effective ratio e).

$$Q_u = q_p\left(1 + e\frac{A_w}{A_p}\right) = \frac{R_p}{d}\left(1 + e\frac{A_w}{A_p}\right) \quad (10)$$

10. Vertical Load Test

10.1 Load test plan

A vertical load test was conducted to clarity the bearing properties of the piles. The test pile was 609.6 mm in the steel pipe body diameter D_o and $1.5D_o$ in the blade diameter, and its screwing was stopped at 13.8 m below the ground level so that its end settled by about $1D_w$ into a sandy layer at a depth of 12.9 m. The load test plan was executed under the Ground Engineering Society Standard "Vertical Load Tests of Piles". The test pile was statistically loaded in multiple cycles in one direction with the load controlled. Another screw pile with excellent pulling performance was used as the reaction pile. The load test schedule is shown in **Table 2**, and the measurement intervals are shown in **Table 3**.

The measurement items were the pile head displacement, pile head strain, pile end strain, and in-pipe soil displacement. The pile end strain gauge was attached to the inside of the steel pipe at $1D_w$ above the pile end and was protected.

Table 2 List of load steps and cycles

cycle	Load step (kN): tf is unit for values enclosed in parentheses
1	490(50)-980(100)-1,960(200)-980(100)-0
2	980(100)-1,960(200)-2,940(300)-3,920(400)-2,940(300)-1,470(150)-0
3	1,960(200)-3,920(400)-4,900(500)-5,880(600)-4,900(500)-2,450(250)-0
4	1,960(200)-3,920(400)-5,880(600)-6,860(700)-7,840(800)-8,820(900)-7,840(800)-3,920(400)-0

Note: Underlined values are initial load.

Table 3 List of load steps and cycles

Load class	Measurement interval (min)
0 load	0-1-2-5-10-15-30
Initial load	0-1-2-5-10-15-30-60
Load within hysteresis loop	0-1-2-5

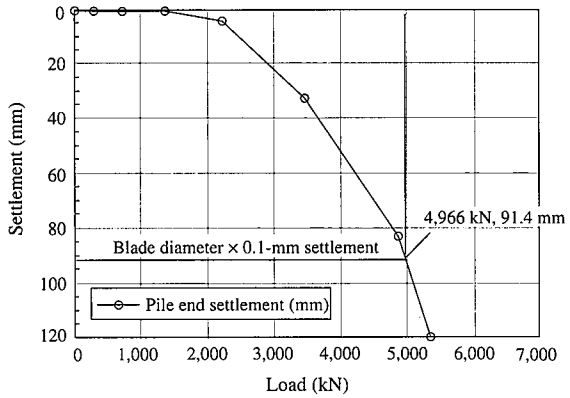

Fig. 14 Pile end load-settlement curve (D = 609.6 mm, $D_w = 1.5D$)

10.2 Vertical load test results

The end load-end penetration curve obtained from the vertical load test is shown in **Fig. 14**. The test pile had extremely large initial stiffness and penetrated drawing a mild arc to a depth equal to 10% of the blade diameter. It then exhibited almost linear under-load penetration behavior and indicated no sudden drop in strength.

When the load at which the pile end penetrated by an amount equal to 10% of the blade diameter is taken as the ultimate load, the ultimate load is 4,966 kN in the vertical load test.

11. Vertical Load Test Results and R_p Value

Of the installation records of the pile used in the load test, the torque, penetration, and applied load are shown in **Figs. 15(a)**, **(b)**, and **(c)**, respectively. The R_p value obtained from the energy equilibrium by using the load test results is shown in **Fig. 15(d)**. As the preconditions to determine the R_p value, the transfer ratio a of L_t and T_t to the pile end and the coefficient α of skin friction between the soil and blade are put at the following values by considering the actual results:

- Transfer ratio of L_t and T_t to pile end: $a = 0.9$
- Coefficient of skin friction between soil and blade: $\alpha = 0.5$

The bit edge resistances Q_{wh} and Q_{wv} are estimated at Q_{wh}, $Q_{wv} = 0$

As a result, R_p was 2,550 kN when the installation of the test pile was stopped. The value of R_p obtained from the force equilibrium is also shown in **Fig. 15(d)**. This value practically agrees with the value of R_p obtained from the energy equilibrium. Since the calculated R_p value is the resistance imposed by the soil on the bottom plate portion of the screw pile, R_p can is considered to reflect the soil conditions in the bottom plate portion of the screw pile.

The end bearing capacity of piles installed by the screw piling method can be expressed by Eq. (10). If e and d are determined, Q_u can be calculated from R_p.

From the equilibrium of forces shown in **Fig. 11**, it is clear that the end uplift capacity Q_{up} is larger than the driving force f_w. Q_{up} can be estimated by

$$Q_{up} \geq R_p - L_b = 2{,}119 \text{ kN}$$

12. Conclusions

The following findings were derived from the results of the full-size pile installation test and vertical load test:

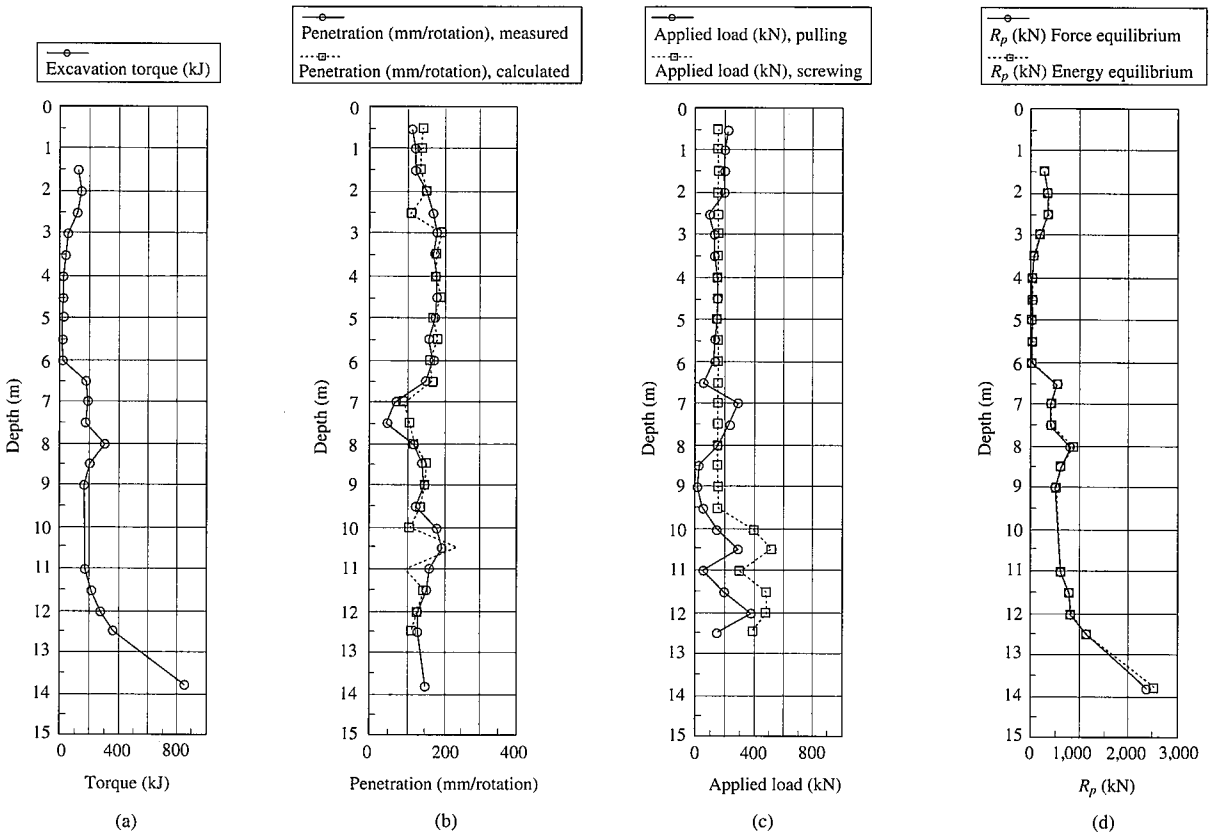

Fig. 15 Installation record and R_p value of load test pile

1) The screw piling method can install medium-diameter screw piles into a sandy layer with an N-value of about 50 to 70. Like their smaller-diameter counterparts, the medium-diameter screw piles can be installed without surplus soil and with low noise and vibration.
2) The blade diameter, angle, and shape have large effects on the installability of screw piles.
3) The soil strength is strongly correlated with the excavation torque. The R_p value proposed here is confirmed to be a factor that can be used to estimate the bearing capacity of screw piles.

13. Future Issues

The following can be cited as future issues:

• Further clarification of mechanism of penetration

The dynamic phenomena occurring at the pile end will be clarified further to find the mechanism of penetration that can explain the penetration of screw piles under all soil conditions.

• Clarification of factors α, a, Q_{wh} and Q_{wv} to derive R_p value and of factors d and e to estimate end bearing capacity

The values given in Chapter 11 were calculated by assuming these factors. The values of these factors will have to be determined by accumulating data through model testing (e.g., with a pressurized sandy ground tank), friction testing, numerical analysis, full-size pipe installation testing, and load testing, among other methods.

• Derivation of equations for estimating end bearing capacity and uplift capacity of screw piles

Postscript

This paper is based on the paper "Study on Screw Steel Pipe Piles" published in the Journal of Structural and Construction Engineering (Vol. 45 B, pp. 453-462, 1999), Architectural Institute of Japan, and contains some revisions made since then.

Acknowledgments

The authors are indebted to people engaged in the development of screw piles for their cooperation in the preparation of this paper.

<Definitions of terms>

Applied dead weight

Dead weight of heavy devices (e.g., a motor) that ride on the pile head.

Applied load

Resultant of the applied dead weight and hold-down load.

Bit edge resistance

Penetration resistance of the soil to which the excavation bit edge is subjected.

Blade

A doughnut disk-shaped steel plate attached to the end of a steel pipe pile. Its shape is spiral or disk-like, and its quantity is one or more.

Blade diameter ratio

Ratio of the blade diameter to the steel pipe body diameter.

Bottom plate

A plate attached to the end of a pile. Used on closed-end piles.

Bottom plate portion

Cross-sectional portion of the end of a filled steel pipe. It is the

"bottom plate" or "bottom plate ring and in-pipe soil portion", and is the projected area portion that offers penetration resistance.

Bottom plate ring
: A doughnut disk-shaped plate attached to the end of a pile. Used on open-end piles. (This term sometimes refers to the internal portion of the blade when the blade extends into the inside of the steel pipe.)

Circle of action
: Circle of action for the resultant of frictional forces used to calculate the torque.

Driving force
: Vertical component of the wedge reaction.

End bearing capacity
: Bearing capacity produced by the bottom plate portion or blade portion.

End uplift capacity
: Resistance produced by the blade to the upward pulling of the pile.

Excavation bit
: A bit attached to the end or lower end of the blade.

Hold-down load
: Vertical load applied to the pile by the hold-down device of a pile driver.

Non-excavation surface
: Ground surface not excavated by the bottom plate portion or blade.

Open-end ratio
: Open area/bottom plate portion area

Opening
: Opening at the pile end (opening in the steel pipe or bottom plate ring)

Penetration
: Amount by which a pile penetrates into the ground during installation.

Penetration force
: Resultant of the applied load and driving force that acts downward on the pile during installation.

Penetration resistance
: Resistance produced by the soil to the bottom plate portion of the pile.

Torque
: Rotating force produced by the motor or twisting force acting on the pile body.

Wedge reaction
: Force acting downward on the pile in the direction normal to the blade when the pile is twisted into the ground during installation.

<Nomenclature>

A_p Projected area of bottom plate portion

A_w Projected area of blade alone

a Transfer ratio of L_t and T_t to pile end ($0 < a < 1$)

D_o Diameter of steel pipe body

D_p' Diameter of circle of action of bottom plate portion = $2D_o/3$

*Torque acting on the infinitesimal width dr on the bottom plate with the radius r is given by

$T_r = 2\pi r \cdot dr \cdot \alpha\sigma r = 2\pi\alpha\sigma r^2 dr$

Integration with respect to the radius R yields

$$T_r = 2\pi\alpha\sigma\int_0^R r^2 dr = 2\pi\alpha\sigma\left[\frac{r^3}{3}\right]_0^R = 2\pi\alpha\sigma\left(R^3/3\right)$$

Resultant of torques on the bottom plate is expressed by

Resultant of torques = $\alpha\sigma \cdot \pi R^2$

From the above equations, the radius of the circle of action in the bottom plate portion is $2R/3$.

D_w Blade diameter

D_w' Diameter of circle of action of blade (circle of action for resultant of forces in rotational direction) = $\dfrac{2\left(D_w^3 - D_o^3\right)}{3\left(D_w^2 - D_o^2\right)}$

*The integration range of the integration equation referred to in the description of D_p' above is $D_o/2$ to $D_w/2$, and the resultant of torque is

Resultant of torque = $\alpha\sigma\pi(D_w^2/4 - D_o^2/4)$

d Penetration resistance reduction factor

e Effective ratio applied to blade bearing capacity

F_p Frictional force acting on bottom plate portion = $\alpha(D_p'/D_w')R_p$

F_w Frictional force acting on upper surface of blade = αP_w

f_w Driving force

H_t Pile end torque replaced by horizontal force on circle of action of blade = $T_b/(D_w'/2)$

K_s Stiffness of soil per unit area when soil is assumed to be elastic-plastic spring

L_b Applied load acting on pile end

L_t Applied load acting on pile head

l Blade length on circle of action

$= \pi D_w' / \cos\theta = \pi D_w' / \sqrt{\left(\pi D_w'\right)^2 + P^2}$

P Blade pitch (axial change in elevation per rotation of blade)

P_o Effective stress in soil at pile end

P_w Wedge reaction

Q_u End bearing capacity of pile

Q_{up} End uplift capacity of pile

Q_{wh} Horizontal bit edge resistance

Q_{wv} Vertical bit edge resistance

Q_{ys} Yield load of soil per unit area when soil is assumed to be elastic-plastic spring

q_p Penetration resistance of bottom plate portion when soil is not disturbed by blade (ultimate bearing capacity)

R_p Penetration resistance of bottom plate portion

S Penetration per rotation

T_b Torque acting on pile end

T_t Torque acting on pile head

α Coefficient of friction between soil and steel plate

η Penetration angle on circle of action

θ Blade angle on circle of action

References

1) Itaya, K., Yoshida, K.: Field Test and Vertical Load Test of Small Diameter Steel Piles with a Steel Helical Blade. Summary of Technical Papers of Annual Meeting, Architectural Institute of Japan. 1986
2) Itaya, K. et al.: Characteristics of Bearing Capacity by Steel Pipe with Tip of Spiral Wing(Part2). Summary of Technical Papers of Annual Meeting, Architectural Institute of Japan. 1990
3) Itaya, K. et al.: Characteristics of Bearing Capacity by Steel Pipe with Tip of Spiral Wing(Part3). Summary of Technical Papers of Annual Meeting, Architectural Institute of Japan. 1990
4) Yamato, S. et al.: Penetration Characteristics of Rotary Penetration of Steel Pile Pipe. 1995, p.1457-1458